31st Annual International Conference of the IEEE EMBS
Minneapolis, Minnesota, USA, September 2-6, 2009

Development of CNT-Based Inductors for Integrated Biosensors

Bruce C. Kim, *Senior Member IEEE*

Abstract—**This paper presents development of Carbon Nanotube based inductors for integrated biosensor applications. Inductors are highly common in RF circuit applications; however, their values and Q factors are limited for today's high-performance RF applications. We describe the design, simulation, and fabrication of Multiwall Carbon Nanotube (MWCNT) based RF inductors, which provide high inductance and Q values that are suitable for wireless integrated biosensors.**

I. INTRODUCTION

CONVENTIONAL RF inductors use spiral-shaped metal on a substrate; they usually have a large footprint with limited inductance and Q values. Using such large-footprint inductors on a silicon substrate, as an example, inhibits adding more transistors on the given silicon area. Carbon nanotubes enable us to replace conventional metal to achieve high-value inductors and quality factors. The values of inductance and quality factors are critical to high-quality RF product design. Current spiral inductors are widely used in many RF circuits in Voltage Controlled Oscillators, as well as in transceivers for cell phones and wireless routers [1, 2, 3, 4]. It is desirable to achieve low power, low phase noise, and wide bandwidth wireless systems with high Q inductors [3].

In this paper we provide design and simulation results for multiwall carbon nanotube (MWCNT) based inductors on silicon, FR-4, and ceramic substrates for wireless biosensor applications. We also provide results from the fabrication of MWCNT-based inductors.

II. CARBON NANOTUBES

Nanotechnology-based package products have recently emerged in the semiconductor industry. Among the nanotechnology-based products on the market, carbon nanotubes are one of the most promising materials for realizing nanoscale inductors. Carbon nanotubes consist of a honeycomb lattice of a graphene sheet rolled into a cylinder. Multiwall CNT (MWCNT) and Single-Wall (SWCNT) are two types of CNT available on the market. They are several micrometers in length and a few nanometers in diameter, resulting in a large aspect ratio that allows approximation of the carbon nanotubes as an ***1D*** system. It is interesting to note that carbon nanotubes can be classified as a metallic or semiconductor; their characteristics can be changed by adjusting the chirality and diameter of CNT.

Pressing or stretching CNTs can change their electrical properties by changing the quantum states of the electrons in the carbon bonds. It is envisaged that one-third of rolled CNTs will be metallic and two-thirds will be semiconductor [5]. Both single-wall and multiwall carbon nanotubes have a low resistivity of approximately150 μΩ.cm. MWCNTs can carry electrical current densities up to 10^{10}A/cm^2 and remain stable for an extended period of time at high temperatures. Although CNTs can carry very high current densities, CNTs on a metal contact may measure high contact resistance in the order of kΩ. The resistivity of CNTs is approximately 10^{-7} Ωm. This makes an ideal material for RF inductors. The high contact resistance between metal and CNTs may be due to weak electronic coupling at the Fermi surface. Metal-CNT contact resistance can be reduced by electron beam bombardment [6] or by using a focused ion beam to deposit metal on CNTs, making it collapse partially and allowing several layers of CNTs to carry current simultaneously; this increases inductances substantially, reduces resistance below 1mΩ, and therefore increases the quality factor Q.

A. Theoretical Derivations

Quantum mechanical effects begin to dominate in nano-scaled carbon nanotubes as their size shrinks. To model carbon nanotubes, we consider kinetic and magnetic inductances. These inductance values are derived from solving both Schrödinger and Boltzmann transport equations. The time-independent Schrödinger equation (Eqn1) in one dimension and the Boltzmann transportation equation (Eqn2) are used to calculate the values of quantum capacitance, quantum (intrinsic) resistance, and kinetic inductance for the spiral inductor made from MWCNT. In steady state, an equal number of electrons are moving in positive and negative ***k*** direction. CNT is an ***1D*** system with limited density of states. With potential applied, the carriers have to move to higher energy states, resulting in an increase in kinetic energy. Extra stored energy results in kinetic inductance. CNTs have two types of capacitance: quantum and electrostatic. The quantum is due to the potential energy variation from state to state.

Manuscript received April 22, 2009. This work was supported in part by the U.S. National Science Foundation under Grant CCF-0541200.
B. C. Kim is with the Department of Electrical & Computer Engineering of University of Alabama, Tuscaloosa, AL 35487 USA (phone: 1-205-348-4972; fax: 1-205-348-6959; e-mail: bruce.kim@ieee.org).

The Boltzmann transport equation is used to analyze transport phenomena within systems that involve density and temperature gradients. The equation is applied to the analysis of the broad spectrum of currents within a system [5, 6]. Solving both the Schrödinger and the Boltzmann transport equations will yield Equations (3), (5), and (6) for kinetic inductances, quantum resistance, and quantum capacitance, respectively.

$$\frac{d^2\psi(x)}{dx^2}+\xi[E]\psi(x)=\xi\lambda\psi(x) \qquad \text{Eqn(1)}$$

$$f(x,v,\phi)=f_0(x,v)-l\cos(\phi)[\frac{\partial f_0}{\partial x}+\frac{a}{v}\frac{\partial f_0}{\partial v}] \qquad \text{Eqn(2)}$$

Assume that there is a time-dependent electric field only in the x direction and confinement in the y and z directions. The kinetic inductance is derived in Equation (3).

$$\mathrm{L}_k=\frac{h}{2e^2v_F} \qquad \text{Eqn(3)}$$

The quantum resistance can be extracted from the partial differential equation in Equation (4).

$$\frac{\partial I}{\partial t}+\frac{I}{\tau}=\frac{e}{L_k}\frac{\partial V}{\partial x} \qquad \text{Eqn(4)}$$

Solving Equation (4) gives us the quantum resistance and capacitance:

$$R_Q=L_k/\tau=\frac{h}{4e^2} \qquad \text{Eqn(5)}$$

$$C_Q=\frac{2e^2}{hv_F} \qquad \text{Eqn(6)}$$

where h is the Planck constant, e is the electron charge, v_F is the Fermi velocity, τ is the relaxation time, L_k is the kinetic inductance, and C_Q is the quantum capacitance.

III. Approach

A conventional integrated inductor is made from aluminum metal with a specific turns ratio, thickness, diameter, and spacing. In this paper the embedded inductor was designed using a multiwall carbon nanotube packaged on silicon, FR-4, and ceramic substrates.

A. Circuit Models for MWCNT Inductors

The inductor is an indispensable part of many RF circuit designs. For example, wireless health monitoring systems, pacemakers and RF ID tags require RF inductors to operate. In RF systems, impedance matching is critical to ensure maximum power transfer from one circuit block to another when two circuit blocks are cascaded. Maximum power transfer is obtained when the output resistance is equal to the input resistance and the output reactive parts are conjugated with the input reactive parts. The equivalent circuit of a two-port spiral inductor is shown in Figures 3 and 4.

A number of lumped element models have been previously published [1, 7]. Some researchers have modeled inductors and analyzed them on a turn-by-turn basis. Others have analyzed inductors on a segment-by-segment basis of the metal. In this paper, our analysis of the CNT inductor will be performed segment by segment on a nanotube.

The CNT spiral inductor discussed in this paper has a 2.5 turns ratio. We used a substrate thickness of 200 microns for silicon and 5 mils for FR-4 and ceramic substrates. The CNT layer on which the inductor is made is separated by a silicon dioxide insulator. The CNT is modeled as series inductance L_x, series resistance R_Q and series feed forward capacitors C_E and C_Q. The two parallel branches represent parasitics on input and output ports. In Figure 2, the capacitor C_{Sub} represents the capacitance between the CNT inductor and the substrate. A similar model for FR-4 and ceramic were derived without Cox as shown in Fig. 2. A series inductance and resistance represent the segment of each CNT inductor. As the different segments are close to each other, there is a mutual inductance between the segments. The mutual inductance and the coupling coefficients between the different self-inductances are calculated by finding the magnetic field inside the spiral CNT segment. These mutual inductances are represented in the model as L_{Mx}.

The circuit model in Figure 2 is unique due to quantum effects such as quantum capacitances and kinetic inductances. Other models that have been discussed in the open literature for CNT are based on transmission lines [7]. Our models take into consideration kinetic and quantum effects that arise from the decrease in size and the high aspect ratio properties of MWCNT.

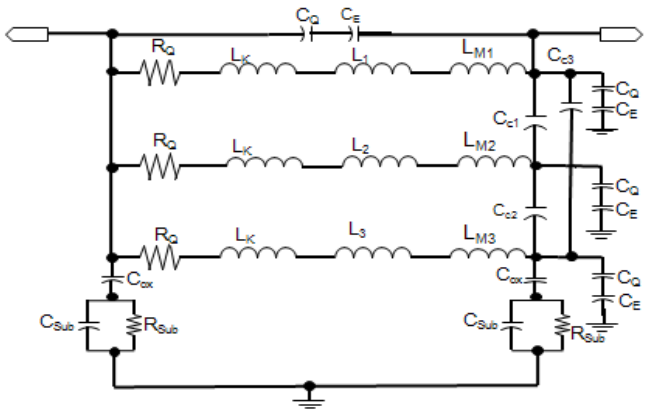

Fig. 2. Equivalent Circuit Model of a Two-Port MWCNT Inductor on a Silicon Substrate.

B. Magnetic Inductances

A simple definition of inductance (L) is the property of a conductor that describes the proportionality between current change and induced voltage. An inductor is any conductor across which there is a voltage drop when a time-varying current is present. Kinetic inductances in MWCNT are

more than four orders of magnitude larger than in metal spiral inductors [6]. Our MWCNT inductor is divided into eleven segments. Each MWCNT segment is 125nm long and 25nm in diameter. The magnetic inductance of each segment can be calculated by considering the MWCNT as a cylinder 25nm in diameter and 125 nm in length. These dimensions have been used in Equation (7) to calculate inductances.

$$L = \frac{\mu_0 l}{2\pi} \ln\left(\frac{d_2}{d_1}\right) \qquad \text{Eqn(7)}$$

C. Electrostatic Capacitance

Capacitance (C) is determined by the length and cross-sectional dimension of MWCNT. The electrostatic capacitance of the MWCNT can be computed using the cylindrical formula for capacitance in Equation (8).

$$C_E = \frac{2\pi\varepsilon}{\ln\left(\frac{y}{d}\right)} \qquad \text{Eqn(8)}$$

While MWCNTs have desirable material properties, individual CNT suffers from a large intrinsic resistance that is not dependent on the length of the CNTs. To alleviate the intrinsic resistance problem, bundles of CNTs have been used [9].

V. Fabrication

We have fabricated a single-wall carbon nanotube (SWCNT) that is approximately 100nm long using the E-beam lithography technique. Figure 4 shows the ultra high-resolution E-beam pattern used to grow carbon nanotubes. These patterns are approximately 18nm in size. The carbon nanotubes are grown in our special CVD (Chemical Vapor Deposition) chamber. Using the same techniques for SWCNT, we have demonstrated the growth of a single MWCNT with 125 nm length and 25nm diameter. The following steps are used to grow MWCNT interconnect:

1. Grow 500nm (nominal) oxide on 3" silicon wafers using PECVD (Plasma Enhanced CVD).
2. Spin-coat wafer with 300nm thick PMMA A4 photoresist at 5000RPM for 60 seconds.
3. Hot-plate bake at 115°C for 60 seconds.
4. E-beam expose at low dose closer to large cross area.
5. Develop 1:1 MIBK in Isopropyl Alcohol (IPA) for 60 seconds.
6. Fix with 90-second soak in IPA.
7. Thermally evaporate the Fe (~0.01gFe).
8. Lift off photo resist using acetone and soak ultrasonic for 30 minutes.
9. Grow carbon nanotubes in the CVD chamber.
10. Use Scanning Electron Microscope (SEM) inspection for close-up views.

In our previous work, we have demonstrated that 100nm long SWCNT interconnect between two 30nm electron beam nickel islands can be developed. These nickel islands were formed by ultra-high resolution electron beam lithography. We have grown the carbon nanotubes in our special CVD chamber. These nickel islands were formed by nanolithography and MWCNT were grown to form spiral shape inductors.

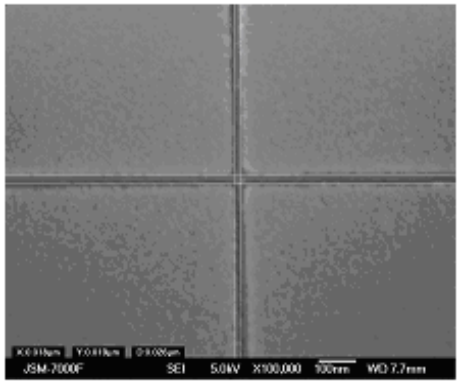

Fig. 4. Sample Electron Beam Lithography Patterns Showing Ultra-High Resolution of Nickel Islands.

Using the process steps described previously, we have grown multiwall carbon nanotubes that can be used to develop MWCNT-based inductors. These MWCNT had physical size of 125nm in length and 25nm in diameter. We were able to grow multiwall carbon nanotubes that had 3 to 5 walls, which made our inductor design more attractive. Multiwall carbon nanotubes have attractive features to reduce the quantum resistance (contact resistance). Figure 6 shows the scanning electron microscopy of the multiwall carbon nanotubes growing from a high-resolution Fe island. We put matrix islands on a substrate so that carbon nanotubes can grow from one island to another as shown in Figure 5. We will be using these carbon nanotube interconnects to develop 2.5 turns ratio CNT-based spiral inductors. To develop a CNT-based inductor with 2.5 turns ratio, we need eleven CNT interconnects in a spiral form.

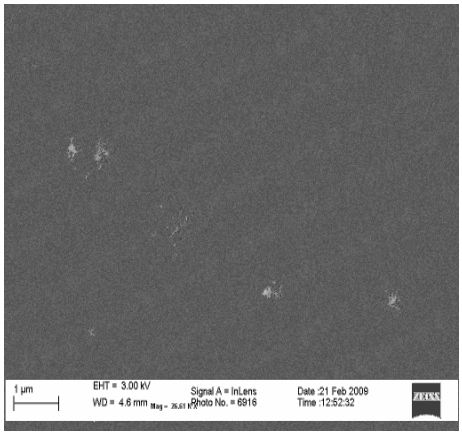

Fig. 6. SEM View of MWCNT to Develop Inductors.

VI. Measurements and Results

We have performed simulations on MWCNT-based inductors for silicon, FR-4, and ceramic substrates. To perform the comparison for different packaging, we have computed the substrate resistance and capacitance. The FR-4 and ceramic substrate resistances are 12GΩ and 1250GΩ, respectively. The resistance of the silicon substrate was much lower, in the range of 100kΩ. The values of electrostatic capacitor C_E of each MWCNT were 15pF. We found coupling capacitances C_{c1} and C_{c2} to be 11pF. However, the coupling capacitance C_{c3} was approximately 6pF. These values were computed from Equation (8). We considered the distance between the walls to be 8nm. The substrate capacitances for silicon, FR-4, and ceramic substrates are 8pF, 6pF, and 3pF, respectively. The quantum capacitance C_Q was computed as 0.2aF for each MWCNT. Using Equation (3), the kinetic inductance L_k was computed as 2nH. The self-inductance for an MWCNT was computed with Equation (7). Their values are 0.028pH. Using the equation $L_M = k\sqrt{L_1 L_2}$, we computed mutual inductances. Their values ranged from 0.008pH to 0.015pH.

In general, the metal-based spiral inductors on Si substrate do not perform as well as the spiral inductors on organic substrate. We have used commercially available software tools to obtain quality factor values. Table I shows quality factors for the MWCNT-based inductor on silicon, FR-4, and ceramic substrates. The quality factor is impressive especially at 5 GHz, where IEEE standard 802.11a is used for wireless telemetry for health monitoring systems. The table shows that a Q factor of 440 was achieved with the silicon substrate, and over 10,000 was possible for ceramic. This indicates that the MWCNT-based inductors have extremely high bandwidth.

TABLE I
CNT-BASED INDUCTOR QUALITY FACTORS FOR SILICON, FR-4, AND CERAMIC SUBSTRATES.

Freq (GHz)	Q on Silicon	Q on FR-4	Q on Ceramic
1	162	1872	3671
2	189	2751	5102
3	297	3812	7766
4	372	4899	9101
5	440	5601	10990

The table indicates that MWCNT-based inductors have very high Q factors. We have simulated self-resonant frequencies of these inductors and they were on the order of terahertz. This provided us with carbon nanotube inductors that can be used in a wide frequency spectrum. From our simulation results, we observed that ceramic substrates provided higher Q factors and inductance values. Figure 7 illustrates inductance values for silicon, FR-4, and ceramic substrates. From the figure, we can observe that the ceramic substrate provided approximately 110nH of inductance at 5GHz. These values seem very useful for today's applications of RF circuit design.

VII. CONCLUSION

This paper provided design and fabrication of multiwall carbon nanotube based RF inductors for integrated biosensors and wireless health monitoring systems. We presented these small footprint inductors on three different substrates. Our simulation results indicate that high quality factors and inductance values can be achieved using carbon nanotubes. This work is highly promising for today's high-performance health monitoring systems and integrated biosensors packaging applications. Therefore, multiwall carbon nanotube based inductors discussed in this paper are the alternative to today's small-footprint inductors.

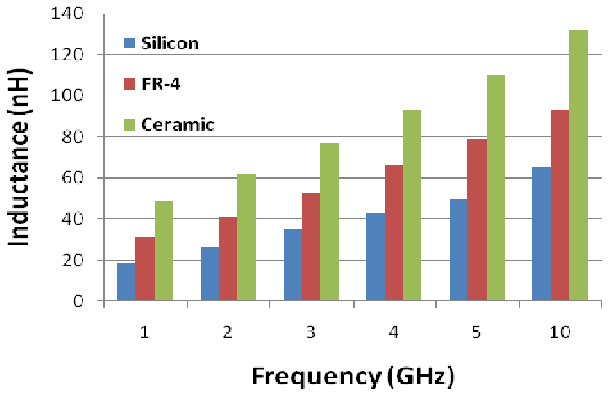

Fig. 7. Inductance Values for Carbon Nanotube Inductors on Silicon, FR-4, and Ceramic Substrates.

ACKNOWLEDGMENT

We would like to acknowledge Dr. Jud Ready's group at Georgia Tech Research Institute for continuous support in CNT synthesis and inductor fabrication.

REFERENCES

[1] N.M Nguyen and R. G. Meyer, "Si IC-Compatible Inductors and LC Passive Filters," IEEE Journal of Solid State Circuits, vol. 25, no. 4, pp. 1028-1030, August 1990.

[2] D. K .Shaeffer and T. H. Lee, "A 1.5-V, 1.5-GHz CMOS low noise amplifier," IEEE Journal of Solid-State Circuits, vol.32, no.5, pp. 745-759, May 1997.

[3] M. D. M. Hershenson, A. Hajimiri, S. S. Mohan, S. P. Boyd and T. H. Lee, "Design and optimization of LC oscillators," 1999 IEEE/ACM International Conference on Computer-Aided Design, Digest of Technical Papers, pp.65-69.

[4] B. Kim, D. Han, R. Liu, "Characterization of On-chip Inductors for Wireless Applications," 59th ARFTG Conference Digest, 2002.

[5] P.J. Burke, "Luttinger liquid theory as a model of the GHz electrical properties of carbon nanotubes", IEEE Transactions on Nanotechnology, vol. 1, no. 3, pp. 129-144, 2002.

[6] A. Bachtold, M. Henny, C. Terrier, et al., "Contacting carbon nanotubes selectively with low-ohmic contacts for four-probe electric measurements," Appl. Phys. Lett., vol. 73 no. 2, pp. 274–276, 1998.

[7] D. Krafesik and D. Dawson, "A Closed–form Expression for Representing the Distributed Nature of the Spiral Inductor," IEEE MTTT Monolithic Circuits Symposium Digest, pp. 87-91, 1986.